MULTIBODY DYNAMICS 2011, ECCOMAS Thematic Conference
J.C. Samin, P. Fisette (eds.)
Brussels, Belgium, 4-7 July 2011

ENERGY-MOMENTUM CONSISTENT INTEGRATION OF FRICTIONAL MULTIBODY CONTACT PROBLEMS

Marlon Franke, Christian Hesch and Peter Betsch

Chair of Computational Mechanics
Department of Mechanical Engineering
University of Siegen, Paul-Bonatz-Str. 9-11, 57076 Siegen
e-mails: franke@imr.mb.uni-siegen.de, hesch@imr.mb.uni-siegen.de,
betsch@imr.mb.uni-siegen.de,
web page: http://www.uni-siegen.de/fb11/nm/

Keywords: Flexible multibody contact, node-to-segment method, mixed method, energy-momentum scheme.

Abstract. *The present work aims at the consistent integration of frictionless as well as frictional flexible multibody contact problems. Therefore a mixed method will be applied on the widely used node-to-segment method. The numerical properties of the energy-momentum time integration scheme based on the concept of a so-called discrete gradient in comparison to the standard midpoint rule will be investigated during a characteristical example.*

1 INTRODUCTION

In the present work we investigate stable integrators for transient large deformation contact problems within the framework of the well known node-to-segment (NTS)-method. For this kind of problem, standard time integrators fail to conserve the total energy of the system. To remedy this drawback, we combine a mixed method with the concept of a discrete gradient applied to the aforementioned NTS-method. The advantage of the energy-momentum scheme is that besides the algorithmic consistency of the angular-momentum the total energy of the system is conserved, leading to a remarkably stable time integration.

In the context of nonlinear elastodynamics various integrators for ordinary differential equations have been extensively developed and investigated during the last three decades (for more details see Ref. [3, 4]). For contact problems, energy consistent integrators have been developed for the NTS-method (see for example Ref. [14, 1, 5]). The concept of the discrete gradient in the sense of Gonzalez (see Ref. [6]) has been applied for the NTS-method (see Ref. [8, 2, 9, 10]). The purpose of the present work is to extend the algorithm from Ref. [10] to frictional three-dimensional contact problems.

To investigate the numerical stability and robustness of our approach, a representative numerical example will be dealt with. To be specific, we consider an impact of a three-dimensional hollow ball with a plate, which stays at rest.

2 Continuum and contact mechanics

To describe large deformation contact problems, we define k bodies $\mathcal{B}^{(i)} \subset \mathbb{R}^3$, $i \in [1, ..., k]$. As illustrated in Fig. (1) we restrict our considerations on a two body problem $i \in [1, 2]$ and exclude selfcontact without prejudice to the generality. The surfaces of both bodies $\partial\mathcal{B}^{(i)}$ are

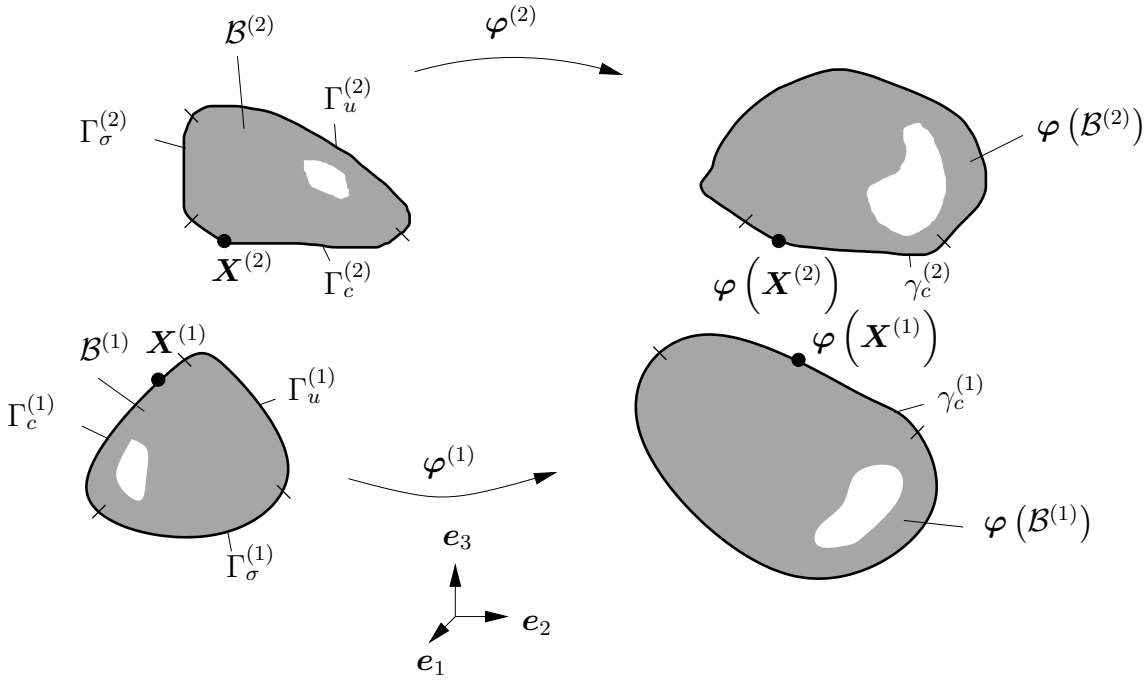

Figure 1: Configurations of two body contact ($\mathcal{B}^i$: bodies in the reference configuration, $\varphi(\mathcal{B}^i)$: bodies in the current configuration)

subdivided into the Dirichlet boundary $\Gamma_u^{(i)}$, the Neumann boundary $\Gamma_\sigma^{(i)}$ and the contact surface

$\Gamma_c^{(i)}$. We assume that the boundaries of each body $\mathcal{B}^{(i)}$ satisfy:

$$\partial\mathcal{B}^{(i)} = \Gamma_\sigma^{(i)} \cup \Gamma_c^{(i)} \cup \Gamma_u^{(i)} \quad \text{and} \quad \Gamma_\sigma^{(i)} \cap \Gamma_c^{(i)} = \Gamma_\sigma^{(i)} \cap \Gamma_u^{(i)} = \Gamma_c^{(i)} \cap \Gamma_u^{(i)} = \emptyset \tag{1}$$

A point of the current configuration within the considered time interval $t \in \mathcal{I} := [0, T]$ can be described by $\boldsymbol{\varphi}(\boldsymbol{X}^{(i)}, t)$. The virtual work of the system reads:

$$\sum_{i=1}^{2} \Bigg(\overbrace{\int_{\mathcal{B}^{(i)}} \rho^{(i)}\, \ddot{\boldsymbol{\varphi}}^{(i)} \cdot \delta\boldsymbol{\varphi}^{(i)}\, \mathrm{d}V}^{=:G^{(i),dyn}} + \overbrace{\int_{\mathcal{B}^{(i)}} \boldsymbol{P}^{(i)} : \nabla_{\boldsymbol{X}}^{(i)}(\delta\boldsymbol{\varphi}^{(i)})\, \mathrm{d}V}^{=:G^{(i),int}}$$

$$\underbrace{- \int_{\mathcal{B}^{(i)}} \rho^{(i)}\, \bar{\boldsymbol{B}}^{(i)} \cdot \delta\boldsymbol{\varphi}^{(i)}\, \mathrm{d}V - \int_{\Gamma_\sigma^{(i)}} \bar{\boldsymbol{T}}^{(i)} \cdot \delta\boldsymbol{\varphi}^{(i)}\, \mathrm{d}A}_{=:G^{(i),ext}} \underbrace{- \int_{\Gamma_c^{(i)}} \boldsymbol{T}^{(i)} \cdot \delta\boldsymbol{\varphi}^{(i)}\, \mathrm{d}A}_{=:G^{(i),c}} \Bigg) = 0 \tag{2}$$

A list of parameters is given in table 1. The first term in equation (2) on the right hand side

$\rho^{(i)}$	:	reference mass density
$\boldsymbol{P}^{(i)}$	:	first Piola-Kirchhoff stress tensor
$\bar{\boldsymbol{B}}^{(i)}$	:	body force per unit volume
$\bar{\boldsymbol{T}}^{(i)}$	:	forces per unit area acting on the Neumann boundary
$\boldsymbol{T}^{(i)}$	:	Piola contact traction

Table 1: List of parameters introduced in equation (2).

contains the inertia forces, where $\ddot{\bullet}$ denotes the second derivative with respect to time. The second term contains the internal forces. The third and fourth term represents the virtual work associated with the body force and surface force, respectively. The last term of equation (2) denotes the contact contribution of the virtual work. In summary, we obtain:

$$\sum_{i=1}^{2} G^{(i)}\left(\boldsymbol{\varphi}, \delta\boldsymbol{\varphi}\right) = \sum_{i=1}^{2} \left(G^{(i),dyn} + G^{(i),int} + G^{(i),ext} + G^{(i),c} \right) = 0 \tag{3}$$

For later developments we focus here on the contact virtual work. Taking the balance of linear momentum into account, we receive (see Ref. [13]):

$$G^c = - \int_{\gamma_c^{(1)}} \boldsymbol{t} \cdot \left(\delta\boldsymbol{\varphi}^{(1)} - \delta\boldsymbol{\varphi}^{(2)} \right)\, \mathrm{d}A \tag{4}$$

Here $\boldsymbol{t}$ denotes the contact traction and $\gamma_c^{(i)} = \boldsymbol{\varphi}(\Gamma_c^{(i)}, t)$ is the contact surface in the current configuration (see also Fig. (1)).

3 Spatial discretization

The bodies are discretized using displacement-based finite elements. Therefore the bodies $\mathcal{B}^{(i)}$ are subdivided into a finite number of elements n_{el}:

$$\mathcal{B}^{(i)} \approx \mathcal{B}^{(i),h} = \bigcup_{e}^{n_{el}} \mathcal{B}_e^{(i),h} \tag{5}$$

We further use the following approximations:

$$\boldsymbol{\varphi}^{(i),h} = \sum_{I=1}^{n_{node}} N_I \, \boldsymbol{x}_I^{(i)}, \quad \delta\boldsymbol{\varphi}^{(i),h} = \sum_{J=1}^{n_{node}} N_J \, \delta\boldsymbol{x}_J^{(i)} \tag{6}$$

Here N_I, N_J denote the shape functions for an eight-node tri-linear brick element. The semi-discrete virtual work for both bodies can now be written as follows:

$$\sum_{i=1}^{2} \left(\overbrace{\int_{\mathcal{B}^{(i),h}} \rho \, N_I \, N_J \, \mathrm{d}V}^{=:M_{IJ}^{(i)}} \ddot{\boldsymbol{x}}_J^{(i)} \cdot \delta\boldsymbol{x}^{(i)} + \overbrace{\int_{\mathcal{B}^{(i),h}} \Big(\nabla N_I(\boldsymbol{X}^{(i)}) \cdot \boldsymbol{S} \Big) \cdot \nabla N_J(\boldsymbol{X}^{(i)}) \, \mathrm{d}V \, \boldsymbol{x}_J^{(i)}}^{=:\boldsymbol{f}^{(i),int}} \cdot \delta\boldsymbol{x}^{(i)} \right.$$

$$\left. \underbrace{- \int_{\mathcal{B}^{(i),h}} N_I \, \rho \, \bar{\boldsymbol{B}} \, \mathrm{d}V \cdot \delta\boldsymbol{x}^{(i)} - \int_{\Gamma_\sigma^{(i),h}} N_I \, \bar{\boldsymbol{T}} \, \mathrm{d}A \cdot \delta\boldsymbol{x}^{(i)}}_{=:\boldsymbol{f}_I^{(i),ext}} \right) + G^{c,h} = 0 \tag{7}$$

where $\boldsymbol{S}$ denotes the second Piola-Kirchhoff stress tensor. The discrete virtual contact work in the current configuration reads:

$$G^{c,h} = - \int_{\gamma_c^{(1),h}} \boldsymbol{t}^h \cdot \big(\delta\boldsymbol{\varphi}_s^{(1),h} - \delta\boldsymbol{\varphi}^{(2),h} \big) \, \mathrm{d}A \tag{8}$$

In summary, we can write:

$$G^h(\boldsymbol{x}, \delta\boldsymbol{x}) = \sum_{i=1}^{2} \delta\boldsymbol{x}_I^{(i)} \, \Big[M_{IJ}^{(i)} \, \ddot{\boldsymbol{x}}_J^{(i)} + \boldsymbol{f}_I^{(i),int} + \boldsymbol{f}_I^{(i),ext} \Big] + G^{c,h} = 0 \tag{9}$$

where $M_{IJ}^{(i)}$ denotes the nodal mass contribution.

3.1 NTS element

For the description of the virtual contact work we use the well known NTS-method (see for example the textbooks Ref. [15, 13]), which uses a slave-master concept (see Ref. [7]). Here we define body $\mathcal{B}^{(1)}$ as slave body and $\mathcal{B}^{(2)}$ as master body. The discrete gap function g_{Ns} denotes the closest point projection from the slave point $\boldsymbol{x}^{(1)}$ to the corresponding master surface represented by $\boldsymbol{x}^{(2)}(\bar{\boldsymbol{\xi}}) = \sum_{K=1}^{4} \hat{N}_K(\bar{\boldsymbol{\xi}}) \, \boldsymbol{x}_K^{(2)}$ (see Fig. (2)). Consistent with the eight-node brick elements used for the isoparametric discretization of the bodies, the shape functions $\hat{N}_K$ are bi-linear and restricted to the contact domain. For the gap function we have to compute the convected coordinates $\bar{\boldsymbol{\xi}}$. Therefore we make use of an additional Newton method solving the following nonlinear problem with respect to $\boldsymbol{\xi}$

$$\begin{bmatrix} \big(\boldsymbol{x}^{(1)} - \boldsymbol{x}^{(2)}(\boldsymbol{\xi}) \big) \cdot \boldsymbol{x}_{,\xi}^{(2)}(\boldsymbol{\xi}) \\ \big(\boldsymbol{x}^{(1)} - \boldsymbol{x}^{(2)}(\boldsymbol{\xi}) \big) \cdot \boldsymbol{x}_{,\eta}^{(2)}(\boldsymbol{\xi}) \end{bmatrix} = \boldsymbol{0} \tag{10}$$

which provides the necessary closest point $\bar{\boldsymbol{\xi}}$ (for more details see the textbook Ref. [15]). Then the gap function can be calculated as follows:

$$g_{Ns} = \left(\boldsymbol{x}_s^{(1)} - \sum_{K=1}^{4} \hat{N}_K(\bar{\boldsymbol{\xi}}) \, \boldsymbol{x}_K^{(2)} \right) \cdot \boldsymbol{n}(\bar{\boldsymbol{\xi}}) \tag{11}$$

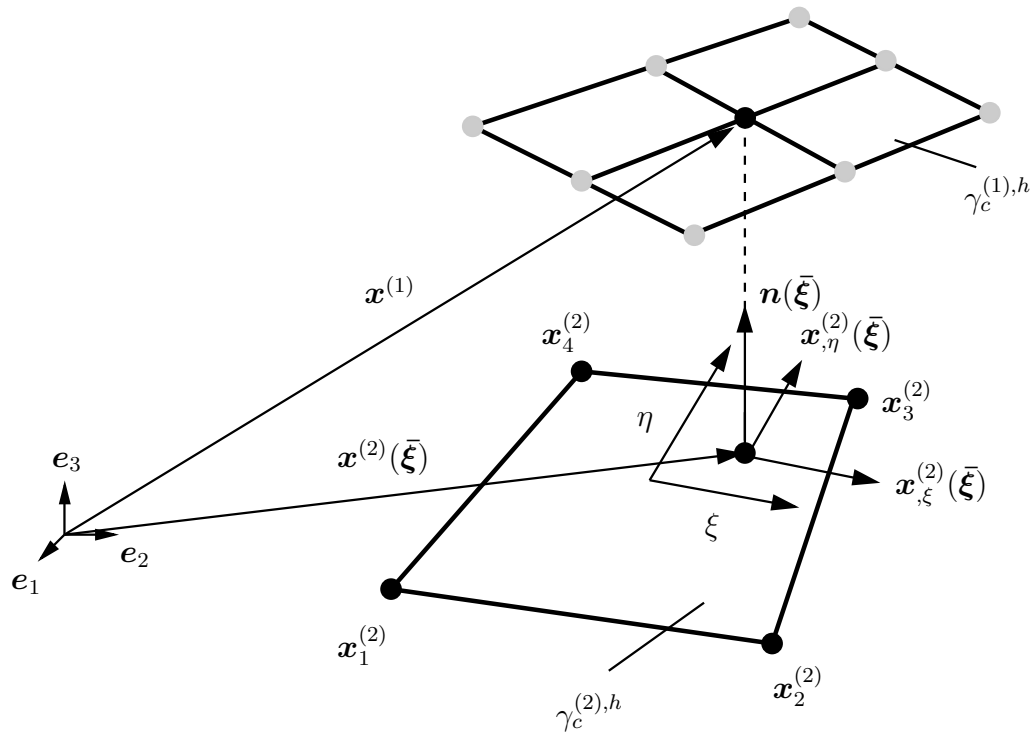

Figure 2: Three-dimensional five node NTS-element.

where $s = 1, ..., n_c$ denotes the sth contact element. The normal $\boldsymbol{n}(\bar{\boldsymbol{\xi}})$ (see Fig. (2)) is defined as:

$$\boldsymbol{n}(\bar{\boldsymbol{\xi}}) = \frac{\boldsymbol{x}_{,\xi}^{(2)}(\bar{\boldsymbol{\xi}}) \times \boldsymbol{x}_{,\eta}^{(2)}(\bar{\boldsymbol{\xi}})}{\|\boldsymbol{x}_{,\xi}^{(2)}(\bar{\boldsymbol{\xi}}) \times \boldsymbol{x}_{,\eta}^{(2)}(\bar{\boldsymbol{\xi}})\|} \tag{12}$$

The NTS-method restrict the gap function such that it remains greater or equal zero. Furthermore the normal tractions are lower or equal zero, hence:

$$g_{Ns} \geq 0, \quad t_{Ns} \leq 0, \quad t_{Ns}\, g_{Ns} = 0 \tag{13}$$

To enforce the above Kuhn-Tucker conditions, there exist different methods. We focus here on the penalty method and on the Lagrange multiplier method. In this connection we divide the contact tractions in equation (4) into a normal and tangential part. Accordingly:

$$G^{c,h} = \int_{\gamma_c^h} \left(t_{Ns}(\bar{\boldsymbol{\xi}})\, \delta g_{Ns}(\bar{\boldsymbol{\xi}}) + \boldsymbol{t}_{Ts} \cdot \delta\bar{\boldsymbol{\xi}} \right) \mathrm{d}A \tag{14}$$

where $\boldsymbol{t}_{Ts}$ represents the frictional traction in tangential direction. The contact pressure in normal direction t_{Ns} for example can be replaced by λ_{Ns} using the Lagrange multiplier and by $\varepsilon_N\, g_{Ns}$ using the penalty method, where $\varepsilon_N > 0$ is a given penalty parameter. For both methods we have to fulfill the Kuhn-Tucker complementary conditions from equation (13) and

one obtains together with the Coulomb friction law:

$$g_{Ns} \geq 0 \tag{15}$$
$$t_{Ns} \leq 0 \tag{16}$$
$$t_{Ns}\, g_{Ns} = 0 \tag{17}$$
$$\Psi_s := \|\boldsymbol{t}_{Ts}\| - \mu\, t_{Ns} \leq 0 \tag{18}$$
$$\boldsymbol{v}_{Ts}^b = \dot{\gamma}\, \frac{\boldsymbol{t}_{Ts}}{\|\boldsymbol{t}_{Ts}\|} \tag{19}$$
$$\dot{\gamma} \geq 0 \tag{20}$$
$$\dot{\gamma}\, \Psi_s = 0 \tag{21}$$

where $\boldsymbol{v}_{Ts}^b$ is the covariant tangential velocity and $\dot{\gamma}$ is the plastic parameter. For the frictionless case we only need to satisfy the conditions (15)-(17). To satisfy the Kuhn-Tucker complementary conditions we make use of an active-set strategy, which separates the set of constraints in an active and an inactive set (see Ref. [12] and the references therein for more details).

3.2 Equation of motion

For the frictionless case we make use of the Lagrange multiplier method. The contact contribution then reads:

$$G^{c,LM} = \sum_{s=1}^{n_c} \lambda_s\, \boldsymbol{n}(\bar{\boldsymbol{\xi}}) \cdot \left(\delta \boldsymbol{x}_s^{(1)} - \sum_{K=1}^{4} \hat{N}_K(\bar{\boldsymbol{\xi}})\, \delta \boldsymbol{x}_K^{(2)} \right) \tag{22}$$
$$\tag{23}$$

where λ_s is the corresponding Lagrange multiplier. To enforce the gap function we use the constraint:

$$\phi_s^{NTS}(\boldsymbol{x}) = g_{Ns} \tag{24}$$

The Lagrangian for the constraint system is:

$$L_\lambda = \frac{1}{2}\, \dot{\boldsymbol{x}} \cdot \boldsymbol{M}\, \dot{\boldsymbol{x}} - V(\boldsymbol{x}) - \sum_{s=1}^{n_c} \phi_s^{NTS}(\boldsymbol{x})\, \lambda_s \tag{25}$$

Using equation (25) we obtain the following semi-discrete index-3 differential algebraic equations:

$$\boldsymbol{M}\, \ddot{\boldsymbol{x}} + \nabla V(\boldsymbol{x}) + \sum_{s=1}^{n_c} \boldsymbol{G}_s^{\mathrm{T}}(\boldsymbol{x})\, \lambda_s = \boldsymbol{0} \tag{26}$$
$$\begin{bmatrix} \phi_1^{NTS} \\ \vdots \\ \phi_{n_c}^{NTS} \end{bmatrix} = \boldsymbol{0} \tag{27}$$

Here $\boldsymbol{G}_s$ is the gradient of the NTS-constraint function with respect to the configuration:

$$\boldsymbol{G}_s^{\mathrm{T}} = \left(\nabla \phi_s^{NTS}(\boldsymbol{x})\right)^{\mathrm{T}} = \begin{bmatrix} \boldsymbol{n}(\bar{\boldsymbol{\xi}}) \\ -N_1\, \boldsymbol{n}(\bar{\boldsymbol{\xi}}) \\ -N_2\, \boldsymbol{n}(\bar{\boldsymbol{\xi}}) \\ -N_3\, \boldsymbol{n}(\bar{\boldsymbol{\xi}}) \\ -N_4\, \boldsymbol{n}(\bar{\boldsymbol{\xi}}) \end{bmatrix} \tag{28}$$

For the frictional case we make use of the penalty method. The contact contribution reads:

$$G^{c,PM} = \sum_{s=1}^{n_c} \left(t_{Ns}(\bar{\boldsymbol{\xi}})\, \delta g_{Ns}(\bar{\boldsymbol{\xi}}) + t_{T\alpha s}\, \delta\bar{\xi}^{\alpha} \right) \tag{29}$$

Note that Einstein summation convention is used. After some algebra the variation of the gap reads:

$$\delta g_{Ns} = \boldsymbol{n}(\bar{\boldsymbol{\xi}}) \, \left(\delta \boldsymbol{x}_s^{(1)} - \delta \boldsymbol{x}^{(2)}(\bar{\boldsymbol{\xi}}) \right) \tag{30}$$

The variation of the convected coordinates finally leads to:

$$\delta\bar{\xi}^{\beta} = [A_{\alpha\beta}]^{-1} \, \left(\left[\delta \boldsymbol{x}_s^{(1)} - \delta \boldsymbol{x}^{(2)}(\bar{\boldsymbol{\xi}}) \right] \, \boldsymbol{x}^{(2)}_{,\alpha}(\bar{\boldsymbol{\xi}}) - g_{Ns}\, \boldsymbol{n}(\bar{\boldsymbol{\xi}})\, \delta \boldsymbol{x}^{(2)}_{,\alpha}(\bar{\boldsymbol{\xi}}) \right) \tag{31}$$

where $A_{\alpha\beta}$ depends on the curvature of the surface ($\boldsymbol{n}(\bar{\boldsymbol{\xi}}) \cdot \boldsymbol{x}^{(2)}_{,\alpha\beta}$):

$$A_{\alpha\beta} = m_{\alpha\beta} + g_{Ns}\, \boldsymbol{n}(\bar{\boldsymbol{\xi}}) \cdot \boldsymbol{x}^{(2)}_{,\alpha\beta} \tag{32}$$

and on the covariant metric:

$$m_{\alpha\beta} = \boldsymbol{x}^{(2)}_{,\alpha} \cdot \boldsymbol{x}^{(2)}_{,\beta} \tag{33}$$

Finally we can write the contact contribution to the residual:

$$\boldsymbol{R}^c_s = t_{Ns}\, \boldsymbol{N}_s + t_{T1s}\, \boldsymbol{D}_{1s} + t_{T2s}\, \boldsymbol{D}_{2s} \tag{34}$$

where the matrices can be calculated as follows:

$$\boldsymbol{D}_{\beta s} = A^{\alpha\beta} \, \left(\boldsymbol{T}_{\alpha} - g_{Ns}\, \boldsymbol{N}_{\alpha} \right) \tag{35}$$

$$\boldsymbol{N}_s = \begin{bmatrix} \boldsymbol{n}(\bar{\boldsymbol{\xi}}) \\ -N_1\, \boldsymbol{n}(\bar{\boldsymbol{\xi}}) \\ -N_2\, \boldsymbol{n}(\bar{\boldsymbol{\xi}}) \\ -N_3\, \boldsymbol{n}(\bar{\boldsymbol{\xi}}) \\ -N_4\, \boldsymbol{n}(\bar{\boldsymbol{\xi}}) \end{bmatrix}, \quad \boldsymbol{T}_{\alpha} = \begin{bmatrix} \boldsymbol{x}^{(2)}_{,\alpha}(\bar{\boldsymbol{\xi}}) \\ -N_1\, \boldsymbol{x}^{(2)}_{,\alpha}(\bar{\boldsymbol{\xi}}) \\ -N_2\, \boldsymbol{x}^{(2)}_{,\alpha}(\bar{\boldsymbol{\xi}}) \\ -N_3\, \boldsymbol{x}^{(2)}_{,\alpha}(\bar{\boldsymbol{\xi}}) \\ -N_4\, \boldsymbol{x}^{(2)}_{,\alpha}(\bar{\boldsymbol{\xi}}) \end{bmatrix}, \quad \boldsymbol{N}_{\alpha} = \begin{bmatrix} \boldsymbol{0} \\ -N_{1,\alpha}\, \boldsymbol{n}(\bar{\boldsymbol{\xi}}) \\ -N_{2,\alpha}\, \boldsymbol{n}(\bar{\boldsymbol{\xi}}) \\ -N_{3,\alpha}\, \boldsymbol{n}(\bar{\boldsymbol{\xi}}) \\ -N_{4,\alpha}\, \boldsymbol{n}(\bar{\boldsymbol{\xi}}) \end{bmatrix} \tag{36}$$

The contravariant contribution $A^{\alpha\beta}$ in equation (35) can be calculated by the inverse of the covariant version of $A_{\alpha\beta}$. Due to equation (34) we obtain the second order ordinary differential equations:

$$\boldsymbol{M}\, \ddot{\boldsymbol{x}} + \nabla V(\boldsymbol{x}) + \sum_{s=1}^{n_c} \boldsymbol{R}^c_s(\boldsymbol{x}) = \boldsymbol{0} \tag{37}$$

3.2.1 Mixed approach

For the frictionless contact we apply an energy-momentum scheme proposed in Ref. [10]. We introduce additional coordinates $\boldsymbol{d}_s \in \mathbb{R}^3$ and the vector $\boldsymbol{f}_s \in \mathbb{R}^3$ which corresponds to the normal $\boldsymbol{n}$ and to the convective coordinates $\boldsymbol{\xi}$ respectively. To determine the augmented

coordinates we introduce augmented constraints to link the new coordinates to the actual configuration. Together with the NTS-constraint we obtain:

$$\boldsymbol{g}_s(\boldsymbol{x}_s, \boldsymbol{d}_s, \boldsymbol{f}_s) = \begin{bmatrix} \phi_s^{NTS} \\ \boldsymbol{\phi}_s^{aug} \end{bmatrix} = \begin{bmatrix} \left(\boldsymbol{x}_s^{(1)} - \boldsymbol{x}^{(2)}(\boldsymbol{f}_s)\right) \cdot \boldsymbol{d}_s \\ \boldsymbol{d}_s \cdot \boldsymbol{x}_{,\xi}^{(2)}(\boldsymbol{f}_s) \\ \boldsymbol{d}_s \cdot \boldsymbol{x}_{,\eta}^{(2)}(\boldsymbol{f}_s) \\ \frac{1}{2}\left(\boldsymbol{d}_s \cdot \boldsymbol{d}_s - 1\right) \\ \left(\boldsymbol{x}_s^{(1)} - \boldsymbol{x}^{(2)}(\boldsymbol{f}_s)\right) \cdot \boldsymbol{x}_{,\xi}^{(2)}(\boldsymbol{f}_s) \\ \left(\boldsymbol{x}_s^{(1)} - \boldsymbol{x}^{(2)}(\boldsymbol{f}_s)\right) \cdot \boldsymbol{x}_{,\eta}^{(2)}(\boldsymbol{f}_s) \end{bmatrix} \tag{38}$$

For more details about the fundamental properties of this formulation we refer to Ref. [10]. With regard to Cauchy's representation theorem, equation (25) can be reparametrized by using at most quadratic invariants $\boldsymbol{\pi}$. One obtains an augmented Lagrangian of the considered system:

$$\tilde{L}_\lambda = \frac{1}{2}\,\dot{\boldsymbol{x}} \cdot \boldsymbol{M}\,\dot{\boldsymbol{x}} - V(\boldsymbol{x}) - \sum_{s=1}^{n_c} \tilde{\boldsymbol{g}}_s(\boldsymbol{\pi}(\boldsymbol{x}_s, \boldsymbol{d}_s, \boldsymbol{f}_s)) \cdot \boldsymbol{\lambda}_s \tag{39}$$

To rewrite the modified NTS constraint in terms of invariants we reformulate them as follows:

$$\begin{aligned} \phi_s^{NTS} &= \left(\boldsymbol{x}_s^{(1)} - \boldsymbol{x}^{(2)}(\boldsymbol{f}_s)\right) \cdot \boldsymbol{d}_s - f_{3s} \\ &= \left(\boldsymbol{x}_s^{(1)} - \left(\boldsymbol{x}_1^{(2)} + \sum_i N_i\,\boldsymbol{x}_i^{(2)} - \sum_i N_i\,\boldsymbol{x}_1^{(2)}\right)\right) \cdot \boldsymbol{d}_s - f_{3s} \\ &= \left(\boldsymbol{x}_s^{(1)} - \boldsymbol{x}_1^{(2)}\right) \cdot \boldsymbol{d}_s - \sum_{i=2}^{4} N_i\,\left(\boldsymbol{x}_i^{(2)} - \boldsymbol{x}_1^{(2)}\right) \cdot \boldsymbol{d}_s - f_{3s} \end{aligned} \tag{40}$$

where f_{3s} is the the third entry of the vector $\boldsymbol{f}_s$. In order to reformulate the constraints we define the following appropriate invariants:

$$\boldsymbol{\pi}(\boldsymbol{x}_s, \boldsymbol{d}_s, \boldsymbol{f}_s) = \begin{bmatrix} \pi_1 \\ \pi_2 \\ \pi_3 \\ \pi_4 \\ \pi_5 \\ \pi_6 \\ \pi_7 \\ \pi_8 \\ \pi_9 \\ \pi_{10} \\ \pi_{11} \\ \pi_{12} \\ \pi_{13} \\ \pi_{14} \\ \pi_{15} \\ \pi_{16} \\ \pi_{17} \end{bmatrix} = \begin{bmatrix} \left(\boldsymbol{x}_s^{(1)} - \boldsymbol{x}_1^{(2)}\right) \cdot \boldsymbol{d}_s \\ \left(\boldsymbol{x}_2^{(2)} - \boldsymbol{x}_1^{(2)}\right) \cdot \boldsymbol{d}_s \\ \left(\boldsymbol{x}_3^{(2)} - \boldsymbol{x}_1^{(2)}\right) \cdot \boldsymbol{d}_s \\ \left(\boldsymbol{x}_4^{(2)} - \boldsymbol{x}_1^{(2)}\right) \cdot \boldsymbol{d}_s \\ f_{1s} \\ f_{2s} \\ f_{3s} \\ \boldsymbol{d}_s \cdot \boldsymbol{d}_s \\ \left(\boldsymbol{x}_2^{(2)} - \boldsymbol{x}_1^{(2)}\right) \cdot \left(\boldsymbol{x}_s^{(1)} - \boldsymbol{x}_1^{(2)}\right) \\ \left(\boldsymbol{x}_3^{(2)} - \boldsymbol{x}_1^{(2)}\right) \cdot \left(\boldsymbol{x}_s^{(1)} - \boldsymbol{x}_1^{(2)}\right) \\ \left(\boldsymbol{x}_4^{(2)} - \boldsymbol{x}_1^{(2)}\right) \cdot \left(\boldsymbol{x}_s^{(1)} - \boldsymbol{x}_1^{(2)}\right) \\ \left(\boldsymbol{x}_2^{(2)} - \boldsymbol{x}_1^{(2)}\right) \cdot \left(\boldsymbol{x}_2^{(2)} - \boldsymbol{x}_1^{(2)}\right) \\ \left(\boldsymbol{x}_2^{(2)} - \boldsymbol{x}_1^{(2)}\right) \cdot \left(\boldsymbol{x}_3^{(2)} - \boldsymbol{x}_1^{(2)}\right) \\ \left(\boldsymbol{x}_2^{(2)} - \boldsymbol{x}_1^{(2)}\right) \cdot \left(\boldsymbol{x}_4^{(2)} - \boldsymbol{x}_1^{(2)}\right) \\ \left(\boldsymbol{x}_3^{(2)} - \boldsymbol{x}_1^{(2)}\right) \cdot \left(\boldsymbol{x}_3^{(2)} - \boldsymbol{x}_1^{(2)}\right) \\ \left(\boldsymbol{x}_3^{(2)} - \boldsymbol{x}_1^{(2)}\right) \cdot \left(\boldsymbol{x}_4^{(2)} - \boldsymbol{x}_1^{(2)}\right) \\ \left(\boldsymbol{x}_4^{(2)} - \boldsymbol{x}_1^{(2)}\right) \cdot \left(\boldsymbol{x}_4^{(2)} - \boldsymbol{x}_1^{(2)}\right) \end{bmatrix} \tag{41}$$

The constraints as a function of the currently defined invariants reads:

$$\tilde{\boldsymbol{g}}_s\left(\boldsymbol{\pi}\left(\boldsymbol{x}_s, \boldsymbol{d}_s, \boldsymbol{f}_s\right)\right) = \begin{bmatrix} \pi_1 - \sum_{i=2}^{4} N_i(\pi_5, \pi_6) \cdot \pi_i - \pi_7 \\ \sum_{i=2}^{4} N_{i,\pi_5}(\pi_5, \pi_6)\, \pi_i \\ \sum_{i=2}^{4} N_{i,\pi_6}(\pi_5, \pi_6)\, \pi_i \\ \frac{1}{2}\left(\pi_8 - 1\right) \\ \sum_{i=2}^{4} N_{i,\pi_5}(\pi_5, \pi_6)\, \pi_{i+6} - \sum_{i=2}^{4} \sum_{j=2}^{4} N_{i,\pi_5}(\pi_5, \pi_6)\, N_j(\pi_5, \pi_6)\, \pi^{LM} \\ \sum_{i=2}^{4} N_{i,\pi_6}(\pi_5, \pi_6)\, \pi_{i+6} - \sum_{i=2}^{4} \sum_{j=2}^{4} N_{i,\pi_6}(\pi_5, \pi_6)\, N_j(\pi_5, \pi_6)\, \pi^{LM} \end{bmatrix} \tag{42}$$

where π^{LM} corresponds to π_{12}-π_{17} according to the assignment of $(\boldsymbol{x}_i^{(2)} - \boldsymbol{x}_1^{(2)}) \cdot (\boldsymbol{x}_j^{(2)} - \boldsymbol{x}_1^{(2)})$ in equation (41). The semi-discrete equations of motion can be obtained by the Lagrangian and

we finally arrive at:

$$\boldsymbol{M}\,\ddot{\boldsymbol{x}} + \nabla V(\boldsymbol{x}) + \sum_{s=1}^{n_c} \left(\mathrm{D}_1\,\boldsymbol{\pi}(\boldsymbol{x}_s, \boldsymbol{d}_s, \boldsymbol{f}_s)\right)^{\mathrm{T}}\,\nabla_{\boldsymbol{\pi}}\tilde{\boldsymbol{g}}_s(\boldsymbol{\pi})\cdot\boldsymbol{\lambda}_s = \boldsymbol{0} \tag{43}$$

$$\sum_{s=1}^{n_c} \left(\mathrm{D}_2\,\boldsymbol{\pi}(\boldsymbol{x}_s, \boldsymbol{d}_s, \boldsymbol{f}_s)\right)^{\mathrm{T}}\,\nabla_{\boldsymbol{\pi}}\tilde{\boldsymbol{g}}_s(\boldsymbol{\pi})\cdot\boldsymbol{\lambda}_s = \boldsymbol{0} \tag{44}$$

$$\sum_{s=1}^{n_c} \left(\mathrm{D}_3\,\boldsymbol{\pi}(\boldsymbol{x}_s, \boldsymbol{d}_s, \boldsymbol{f}_s)\right)^{\mathrm{T}}\,\nabla_{\boldsymbol{\pi}}\tilde{\boldsymbol{g}}_s(\boldsymbol{\pi})\cdot\boldsymbol{\lambda}_s = \boldsymbol{0} \tag{45}$$

$$\begin{bmatrix} \tilde{\boldsymbol{g}}_1(\boldsymbol{\pi}(\boldsymbol{x}_1, \boldsymbol{d}_1, \boldsymbol{f}_1)) \\ \vdots \\ \tilde{\boldsymbol{g}}_{n_c}(\boldsymbol{\pi}(\boldsymbol{x}_{n_c}, \boldsymbol{d}_{n_c}, \boldsymbol{f}_{n_c})) \end{bmatrix} = \boldsymbol{0} \tag{46}$$

Again we refer to Ref. [10] for the derivation of the fundamental properties of the constraints and for the verification of the conservation of the angular momentum $\boldsymbol{J} = \sum_{I,J} M_{I,J}\,\boldsymbol{x}_I \times \dot{\boldsymbol{x}}_J$ as well as of the total energy $E(\boldsymbol{x}, \dot{\boldsymbol{x}}) = \frac{1}{2}\,\dot{\boldsymbol{x}}\cdot\boldsymbol{M}\,\dot{\boldsymbol{x}} + V(\boldsymbol{x})$ of the semi-discrete system.

4 Time discretization

For the time discretization we divide the time interval $\mathcal{I} = [0, T] = \bigcup_{n=0}^{N-1}[t_n, t_{n+1}]$ into equidistant increments $h = t_{n+1} - t_n$ to apply an one step time integration scheme. In the following the time discretization according to frictionless and frictional contact will be stated.

4.1 Frictionless contact with Lagrange multipliers

For later comparison we apply a standard midpoint rule and a newly developed energy-momentum scheme (firstly presented in Ref. [10]) in order to investigate the numerical properties of the latter.

Midpoint rule For the midpoint rule the configuration, velocity and acceleration are evaluated in the midpoint:

$$\boldsymbol{x}_{n+\frac{1}{2}} = \frac{1}{2}\,(\boldsymbol{x}_{n+1} + \boldsymbol{x}_n) \tag{47}$$

$$\boldsymbol{v}_{n+\frac{1}{2}} = \frac{1}{h}\,(\boldsymbol{x}_{n+1} - \boldsymbol{x}_n) \tag{48}$$

$$\boldsymbol{a}_{n+\frac{1}{2}} = \frac{2}{h^2}\,(\boldsymbol{x}_{n+1} - \boldsymbol{x}_n) - \frac{2}{h}\,\boldsymbol{v}_n \tag{49}$$

By applying the midpoint rule along with the equations (26) and (27) we finally obtain the completely discrete equations:

$$\boldsymbol{x}_{n+1} - \boldsymbol{x}_n - h\,\boldsymbol{v}_{n+\frac{1}{2}} = \boldsymbol{0} \tag{50}$$

$$\boldsymbol{M}\,(\boldsymbol{v}_{n+1} - \boldsymbol{v}_n) + h\,\left(\nabla V(\boldsymbol{x}_{n+\frac{1}{2}}) + \sum_{s=1}^{n_c} \boldsymbol{G}_s^{\mathrm{T}}(\boldsymbol{x}_{n+\frac{1}{2}})\,\lambda_{s,n+1}\right) = \boldsymbol{0} \tag{51}$$

$$\begin{bmatrix} \phi_{1,n+1}^{NTS} \\ \vdots \\ \phi_{n_c,n+1}^{NTS} \end{bmatrix} = \boldsymbol{0} \tag{52}$$

Note that we use Newton's method to solve the problem and we have to calculate the tangent.

Energy-momentum scheme - mixed formulation We aim at the time discretization for the mixed formulation (see Section 3.2.1), where the NTS constraints are reformulated in appropriate invariants. Further we introduce a discrete gradient in the sense of Gonzalez (see Ref. [6]). This creates an energy-momentum scheme which besides the algorithmic consistency of both momentum maps is able to conserve the total energy of the system. Finally we can write the completely discrete system within the concept of the discrete gradient as follows:

$$\boldsymbol{x}_{n+1} - \boldsymbol{x}_n - h\,\boldsymbol{v}_{n+\frac{1}{2}} = \boldsymbol{0} \tag{53}$$

$$\boldsymbol{M}\ (\boldsymbol{v}_{n+1} - \boldsymbol{v}_n) + h\,\overline{\nabla}_{\boldsymbol{x}}\, V(\boldsymbol{x}_n, \boldsymbol{x}_{n+1}) \tag{54}$$

$$+h\sum_{s=1}^{n_c}\left(\mathrm{D}_1\,\boldsymbol{\pi}(\boldsymbol{x}_{s,n+\frac{1}{2}}, \boldsymbol{d}_{s,n+\frac{1}{2}}, \boldsymbol{f}_{s,n+\frac{1}{2}})\right)^{\mathrm{T}}\,\overline{\overline{\nabla}}_{\boldsymbol{\pi}}\,\tilde{\boldsymbol{g}}_s(\boldsymbol{\pi}_n, \boldsymbol{\pi}_{n+1})\cdot\boldsymbol{\lambda}_{s,n+1} = \boldsymbol{0} \tag{55}$$

$$\sum_{s=1}^{n_c}\left(\mathrm{D}_2\,\boldsymbol{\pi}(\boldsymbol{x}_{s,n+\frac{1}{2}}, \boldsymbol{d}_{s,n+\frac{1}{2}}, \boldsymbol{f}_{s,n+\frac{1}{2}})\right)^{\mathrm{T}}\,\overline{\overline{\nabla}}_{\boldsymbol{\pi}}\,\tilde{\boldsymbol{g}}_s(\boldsymbol{\pi}_n, \boldsymbol{\pi}_{n+1})\cdot\boldsymbol{\lambda}_{s,n+1} = \boldsymbol{0} \tag{56}$$

$$\sum_{s=1}^{n_c}\left(\mathrm{D}_3\,\boldsymbol{\pi}(\boldsymbol{x}_{s,n+\frac{1}{2}}, \boldsymbol{d}_{s,n+\frac{1}{2}}, \boldsymbol{f}_{s,n+\frac{1}{2}})\right)^{\mathrm{T}}\,\overline{\overline{\nabla}}_{\boldsymbol{\pi}}\,\tilde{\boldsymbol{g}}_s(\boldsymbol{\pi}_n, \boldsymbol{\pi}_{n+1})\cdot\boldsymbol{\lambda}_{s,n+1} = \boldsymbol{0} \tag{57}$$

$$\begin{bmatrix} \tilde{\boldsymbol{g}}_1(\boldsymbol{\pi}(\boldsymbol{x}_{1,n+1}, \boldsymbol{d}_{1,n+1}, \boldsymbol{f}_{1,n+1})) \\ \vdots \\ \tilde{\boldsymbol{g}}_{n_c}(\boldsymbol{\pi}(\boldsymbol{x}_{n_c,n+\frac{1}{2}}, \boldsymbol{d}_{n_c,n+\frac{1}{2}}, \boldsymbol{f}_{n_c,n+\frac{1}{2}})) \end{bmatrix} = \boldsymbol{0} \tag{58}$$

Here the discrete gradient $\overline{\nabla}_{\boldsymbol{x}}\, V(\boldsymbol{x}_n, \boldsymbol{x}_{n+1})$ applied to the internal energy is used (for more details see Ref. [3]). In addition, the discrete gradient $\overline{\overline{\nabla}}_{\boldsymbol{\pi}}\,\tilde{\boldsymbol{g}}(\boldsymbol{\pi}_n, \boldsymbol{\pi}_{n+1})$ is defined as follows:

$$\overline{\overline{\nabla}}_{\boldsymbol{\pi}}\,\tilde{\boldsymbol{g}}_s(\boldsymbol{\pi}_n, \boldsymbol{\pi}_{n+1}) = \nabla_{\boldsymbol{\pi}}\,\tilde{\boldsymbol{g}}_s\left(\boldsymbol{\pi}_{n+\frac{1}{2}}\right)$$
$$+\frac{\tilde{\boldsymbol{g}}_s(\boldsymbol{\pi}_{n+1}) - \tilde{\boldsymbol{g}}_s(\boldsymbol{\pi}_n) + \nabla_{\boldsymbol{\pi}}\,\tilde{\boldsymbol{g}}_s\left(\boldsymbol{\pi}_{n+\frac{1}{2}}\right)\,(\boldsymbol{\pi}_{s,n+1} - \boldsymbol{\pi}_{s,n})}{\|\boldsymbol{\pi}_{s,n+1} - \boldsymbol{\pi}_{s,n}\|^2}\,(\boldsymbol{\pi}_{s,n+1} - \boldsymbol{\pi}_{s,n}) \tag{59}$$

The verification of the conservation of the angular momentum and the total energy of the completely discrete system can be found in Ref. [10]. To this end we have to remark that the consistency condition is violated in general by an inactive constraint, which gets active within a specific time step.

4.2 Frictional contact with penalty method

For frictional contact we apply the penalty method. Therefore we have to distinguish whether stick ($\Psi \leq 0$) or slip ($\Psi > 0$) occurs. To this end usually a return mapping scheme (for more details see Ref. [13] and Ref. [15]) is implemented that works as follows. One first assumes stick and computes therefore a trial state during the increment:

$$t^{trial}_{T\alpha,n+1} = t_{T\alpha,n} + \varepsilon_T\, m_{\alpha\beta}\,\left(\bar{\xi}^{\beta}_{n+1} - \bar{\xi}^{\beta}_{n}\right) \tag{60}$$

$$\Psi^{trial}_{n+1} = \|\boldsymbol{t}^{trial}_{T,n+1}\| - \mu\, t_{N,n+1} \tag{61}$$

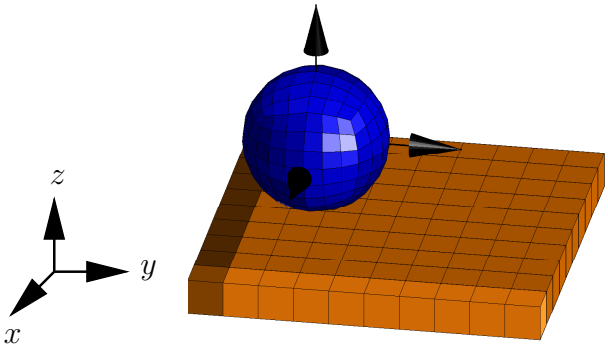

Figure 3: Initial configuration of the hollow ball and plate.

Here μ is the Coulomb coefficient of friction. On the basis of the slip condition Ψ_{n+1}^{trial} the frictional tractions $t_{T\alpha,n+1}$ will be computed:

$$t_{T\alpha,n+1} = \begin{cases} t_{T\alpha,n+1}^{trial} & \text{if } \Psi_{n+1}^{trial} \leq 0 \quad \text{(stick)} \\ \mu\, t_{N,n+1} \frac{t_{T\alpha,n+1}^{trial}}{\|\boldsymbol{t}_{T,n+1}^{trial}\|} & \text{if } \Psi_{n+1}^{trial} > 0 \quad \text{(slip)} \end{cases} \tag{62}$$

Then equation (37) can be evaluated in the midpoint due to equations (47)-(49). Finally one obtains the following completely discrete equations of motion:

$$\boldsymbol{x}_{n+1} - \boldsymbol{x}_n - h\, \boldsymbol{v}_{n+\frac{1}{2}} = \boldsymbol{0} \tag{63}$$

$$\boldsymbol{M}\ (\boldsymbol{v}_{n+1} - \boldsymbol{v}_n) + h \left(\nabla V(\boldsymbol{x}_{n+\frac{1}{2}}) + \sum_{s=1}^{n_c} \boldsymbol{R}_s^c(\boldsymbol{x}_{n+\frac{1}{2}}) \right) = \boldsymbol{0} \tag{64}$$

5 Numerical examples

As numerical example we consider the impact of a hollow ball with a plate. The initial configuration is displayed in Fig. 3. At the start the velocity of the hollow ball is $v_x = 0$, $v_y = 1$, $v_z = -1$ where the plate stays at rest. Both bodies are modeled with a St. Venant-Kirchhoff material and with a Poisson's ratio of $\nu = 0.4$. The Young's modulus of both bodies is $E = 10^5$. The hollow ball is discretized with 432 and the plate with 100 eight-node brick elements.

For the frictionless contact of the example shown in Fig. 3 we compare the midpoint rule with the proposed energy-momentum scheme. We use a time step size of $h = 0.01$ during

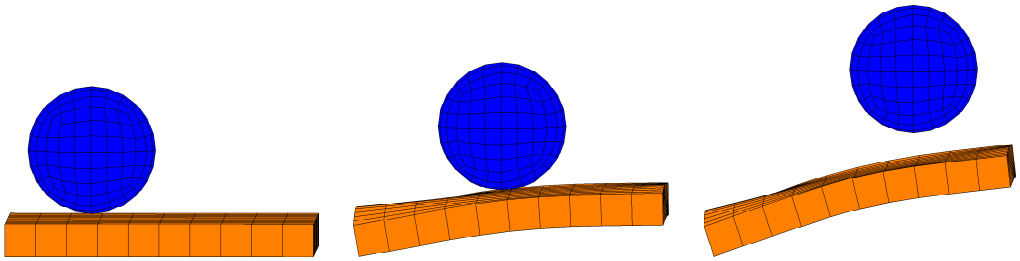

Figure 4: Snapshots for the midpoint rule at time $t = 0.0$ (left), $t = 0.5$ (middle) and $t = 1.0$ (right).

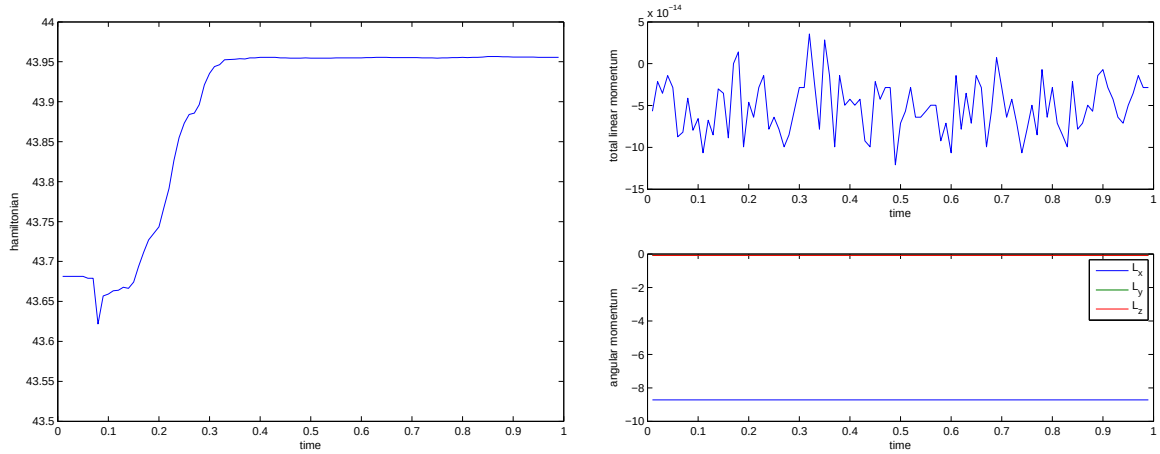

Figure 5: Energy plot (left), total linear momentum (top right) and angular momentum (bottom right) corresponding to the midpoint rule.

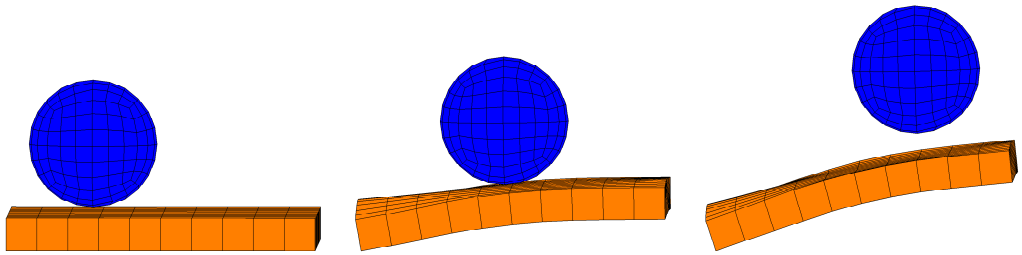

Figure 6: Snapshots for the energy-momentum scheme at time $t = 0.0$ (left), $t = 0.5$ (middle) and $t = 1.0$ (right).

the interval $\mathcal{I} = [0, 1]$ for both simulations. No external forces and momenta are acting on the bodies, so we consider the system as a conservative system, which means that the basic properties of the bodies, namely the total energy, the angular as well as the linear momentum, have to be conserved. In Fig. 5 and Fig. 7 the basic properties of both bodies are displayed for the midpoint rule and the energy-momentum scheme, respectively. Three snapshots at times $t = 0.0$, $t = 0.5$ and $t = 1.0$ for both simulations are displayed in Fig. 4 and Fig. 6. It becomes obvious that the energy-momentum scheme (see Fig. 7) conserves all quantities whereas the midpoint rule (see Fig. 5) fails to conserve the energy.

6 CONCLUSIONS

- As a new approach a mixed method together with an energy-momentum scheme has been applied to three-dimensional contact problems described by the NTS-method.
- For the mixed method augmented coordinates and additional constraints were introduced. Then the constraints were reparametrized by appropriate invariants.
- Further the concept of the discrete gradient has been applied on the internal energy and on the contact constraints.
- As shown the method can be extended to frictional contact problems as well.

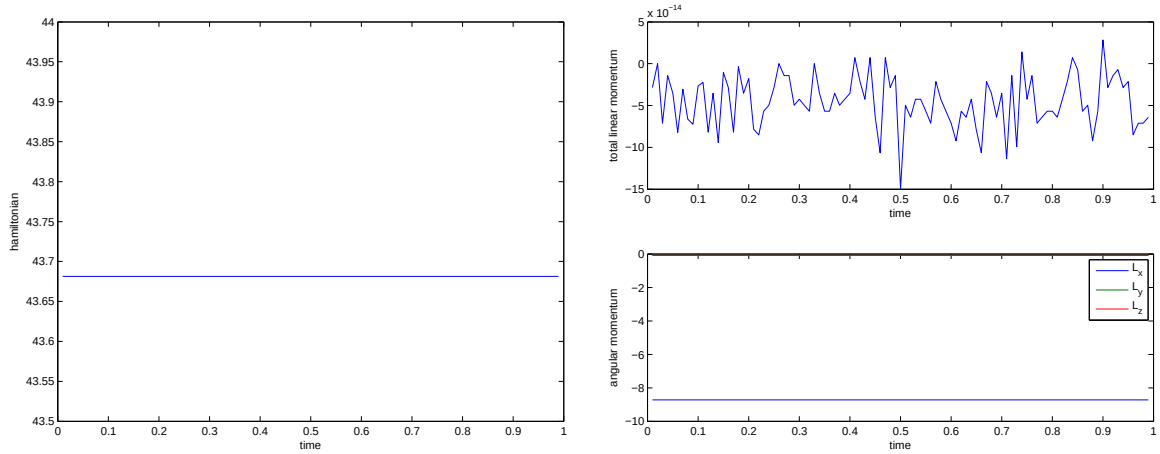

Figure 7: Energy plot (left), total linear momentum (top right) and angular momentum (bottom right) corresponding to the energy-momentum scheme.

- The properties of the energy-momentum scheme has been numerically investigated in comparison to the midpoint rule.
- In summary, the newly developed method results in a highly stable integration scheme.

REFERENCES

[1] F. Armero and E. Petöcz, Formulation and analysis of conserving algorithms for frictionless dynamic contact/impact problems, *Comput. Methods Appl. Mech. Engrg.*, **158**, 269–300, 1998.

[2] P. Betsch and C. Hesch, Energy-momentum conserving schemes for frictionless dynamic contact problems. Part I: NTS method. In P. Wriggers and U. Nackenhorst, editors, *IUTAM Symposium on Computational Methods in Contact Mechanics*, volume 3 of IUTAM Bookseries, pages 77–96. Springer-Verlag, 2007.

[3] P. Betsch and P. Steinmann, Conservation properties of a time FE method. Part II: Timestepping schemes for nonlinear elastodynamics. *Int. J. Numer. Meth. Engng*, **50**, 1931–1955, 2001.

[4] P. Betsch and P. Steinmann, Conservation properties of a time FE method. Part III: Mechanical systems with holonomic constraints. *Int. J. Numer. Meth. Engng*, **53**, 2271–2304, 2002.

[5] V. Chawla and T.A. Laursen, Energy consistent algorithms for frictional contact problems. *Int. J. Numer. Meth. Engng*, **42**(5), 799–827, 1998.

[6] O. Gonzalez, *Design and analysis of conserving integrators for nonlinear Hamiltonian systems with symmetry*. Ph.D. Thesis, Department of Mechanical Engineering, Stanford University, 1996.

[7] J.O. Hallquist, NIKE2D: An implicit, finite-deformation, finite-element code for analyzing the static and dynamic response of two-dimensional solids. *Technical Report UCRL-52678*, Lawrence Livermore Laboratory, Livermore, CA, 1979.

[8] P. Hauret and P. Le Tallec, Energy-controlling time integration methods for nonlinear elastodynamics and low-velocity impact. *Comput. Methods Appl. Mech. Engrg.*, **195**, 4890–4916, 2006.

[9] C. Hesch, *Mechanische Integratoren für Kontaktvorgänge deformierbarer Körper unter großen Verzerrungen*. Ph.D. Thesis, Department of Mechnical Engineering, University of Siegen, 2007.

[10] C. Hesch and P. Betsch, Transient 3d contact problems – NTS method: Mixed methods and conserving integration, *Computational Mechanics*, DOI: 10.1007/s00466-011-0597-2

[11] G.A. Holzapfel, *Nonlinear solid mechanics*. John Wiley & Sons, 2000.

[12] S. Hüeber and B.I. Wohlmuth, A primal-dual active set strategy for non-linear multibody contact problems. *Comput. Methods Appl. Mech. Engrg.*, **194**, 3147–3166, 2005.

[13] T.A. Laursen, *Computational contact and impact mechanics*. Springer-Verlag, 2002.

[14] T.A. Laursen and V. Chawla, Design of energy conserving algorithms for frictionless dynamic contact problems. *Int. J. Numer. Meth. Engng*, **40**, 863–886, 1997.

[15] P. Wriggers, *Computational contact mechanics*. Springer-Verlag, 2nd edition, 2006.